Journal of Nuclear Materials 400 (2010) 196–204

Contents lists available at ScienceDirect

Journal of Nuclear Materials

journal homepage: www.elsevier.com/locate/jnucmat

Numerical modeling of oxygen diffusion in the wall thickness of Low-Tin Zircaloy-4 fuel cladding tube during high temperature (1100–1250 °C) steam oxidation

C. Corvalán-Moya [a], C. Desgranges [a], C. Toffolon-Masclet [a,*], C. Servant [b], J.C. Brachet [a]

[a] CEA, Nuclear Materials Department, 91191 Gif-sur-Yvette Cedex, France
[b] Université de Paris-Sud, Laboratoire de Physico-Chimie de l'Etat Solide, ICMMO, 91405 Orsay, France

ARTICLE INFO

Article history:
Received 27 October 2009
Accepted 4 March 2010

ABSTRACT

A new numerical tool has been developed by coupling the diffusion code "EKINOX" (Estimation Kinetics Oxidation) and the thermodynamic database "ZIRCOBASE" using TQ (ThermoCalc program interface). The aim of this tool is to calculate the oxygen diffusion during oxidation of Zr based alloys. The simulation results of the oxide growth kinetics and the induced oxygen diffusion profiles in the [1100–1250 °C] temperature range, at different times, are presented and compared to previous experimental results. An estimation of the diffusion coefficient in the α phase is deduced from this comparison. The results are discussed in comparison to previous models based on an analytical treatment and the influence of the choice of the thermodynamic data set on the final oxygen diffusion profile is explored.

Finally, it is shown that the present modeling is able to predict quite accurately the "critical" oxidation time corresponding to the overall ductile-to-brittle transition of the high temperature (HT) oxidized clad.

1. Introduction

During some hypothetical Pressurized Water Reactor (PWR) accidental scenario such as Loss of Coolant Accident (LOCA), the nuclear fuel cladding tubes made of Zr base alloys are subjected to a high temperature (HT) oxidation (up to ~1200 °C) caused by the steam environment. This leads to the growth of a zirconia layer (ZrO_2), but also to the growth of $\alpha_{Zr(O)}$ phase from the parent (ductile) β_{Zr} phase due to the oxygen diffusion within the sub-oxide metallic layer (see Fig. 1). The zirconia and the $\alpha_{Zr(O)}$ phase layers are brittle at low temperatures, then, the residual ductility of the HT oxidized cladding tube depends mainly on the oxygen concentration in the prior β_{Zr} phase inner layer. It has been recently demonstrated by Brachet et al. [1], from room temperature (RT) impact test data, that the post-quench (PQ) ductile-to-brittle transition within the prior-β layer occurs locally for a critical oxygen concentration value closed to 0.4 wt.% (Fig. 2). Kim et al. [2] have reached similar conclusions by performing different experimental simulations of LOCA tests. The failure behavior of the Zircaloy-4 cladding was evaluated by 3-point absorbed energy tests. An oxygen content less than 0.5 wt.% in the β phase was corroborated to maintain the cladding ductility after the LOCA test. Thus, knowing accurately the kinetics growth of the $\alpha_{Zr(O)}$ phase and the oxygen concentration profiles in the β_{Zr} phase are a key issue to predict the amount of ductile phase remaining in the cladding tube after a LOCA scenario. Analytical oxygen diffusion models [3], used previously, are limited to semi-infinite samples, consequently, the oxygen concentration prediction in the β phase and the simulation of the $\beta \rightarrow \alpha$ phase transformation need to be improved. Thus, in order to predict accurately the amount of oxygen in prior β_{Zr} phase, a new tool is being developed. This tool results from the coupling between the ZIRCOBASE [4] (thermodynamic database) and an adaptation of the EKINOX numerical code [5], originally developed for Ni alloy [6].

In a first part of this paper, the context of this work and the diffusion–reaction model are presented. Then, a description of the numerical tool is shown. In the second part, the oxygen profiles are simulated at different times and compared to previous experimental data [1], in the temperature range 1100–1250 °C.

2. Framework

The solid–solid phase transformations and the microstructural changes due to basic diffusive processes occurring upon HT transients, such as LOCA accident, are of fundamental interest to evaluate the post-quench (PQ) mechanical properties of the HT oxidized fuel cladding tubes.

The first oxygen embrittlement criteria in Zy-4 fuel cladding were introduced by Sawatzky [7]. This author proposed a brittle failure mode when half of the cladding tubes exceeded 0.7 wt.% oxygen content.

Extensive studies were carried out to precisely evaluate the oxidation rate of Zircaloy in a high temperature steam for a LOCA safety analysis. Baker et al. [8] obtained a temperature dependence for the oxidation parabolic rate above 1000 °C, that has been used

* Corresponding author. Tel.: +33 1 69082139.
E-mail address: caroline.toffolon@cea.fr (C. Toffolon-Masclet).

0022-3115/$ - see front matter © 2010 Elsevier B.V. All rights reserved.
doi:10.1016/j.jnucmat.2010.03.004

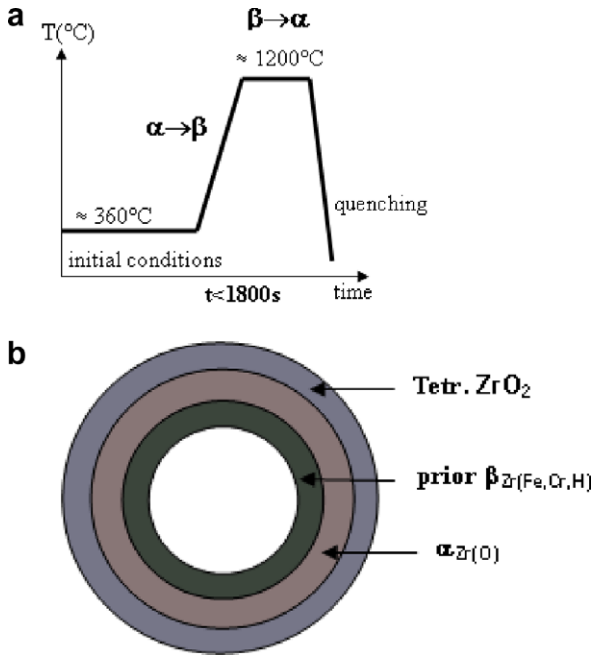

Fig. 1. Simplified LOCA transient (a) and scheme of the clad after HT oxidation and quenching (b).

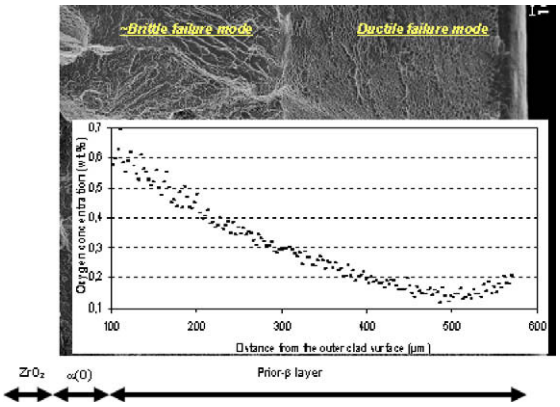

Fig. 2. Typical prior-β fractograph of an impact tested Zircaloy-4 sample at 20 °C and associated oxygen diffusion profile after steam oxidation for 120 s at 1250 °C and quenching (from [1]).

as the safety criteria of the high temperature oxidation for the Zr cladding materials. Urbanic et al. [9] studied the oxidation kinetics of zirconium alloys in the temperature range 1050–1850 °C by the hydrogen evolution and the weight gain methods. A parabolic kinetic (indicating a diffusion controlled reaction mechanism) was corroborated but the parabolic rate constants were inferior to those given by Baker et al. [8] in the Arrhenius plot over the temperature range 1050–1580 °C. In a similar temperature range, 927–1370 °C, Hobson et al. [10] measured the parabolic constant oxidations by determining the zirconia thickness. These results are in good agreement with the work of Urbanic et al. [9].

Ocken et al. [11,12] compared isothermal oxidation kinetics of Zirconium alloys and different parabolic rate constants were found. The discrepancy between these results is explained by the different procedures used to heat the specimens (induction heating or resistive heating).

Brachet et al. [13] have made an accurate quantification of the α(O) and prior-β phases amount in Zr alloys during high temperatures oxidation and the oxidation parabolic rate constants were determined. As mentioned above, Brachet et al. [1] demonstrated by fractographic examinations and evaluation of failure mode that the cooling scenario has a significant impact on the post-quench mechanical properties. The hydrogen and oxygen content were determined by nuclear and electron microprobes measurements. A critical oxygen concentration close to 0.4 wt.% was found for the ductile-to-brittle transition.

Thus, it is a key issue to anticipate changes in the cladding wall during thermal LOCA transient such as presented in the Fig. 1. In the first stage, that is normal conditions, the fuel claddings operate at around 360 °C, where α_{Zr} is the stable metallic phase. Also at this "low temperature" a thin layer of monoclinic zirconium oxide, with a reduced growing rate, covers the α_{Zr} matrix. At this temperature, the atomic movements are too slow to initiate meaningful changes in the physico-chemical features, like a phase transformation in the substrate.

On the contrary, during the transitory stage of LOCA, when the cladding reaches higher temperatures, the solubility and the diffusive process of oxygen into the sub-oxide alloy becomes significant and promotes oxygen diffusion inside the sub-oxide metallic part of the cladding tube. For oxidizing temperatures above ~900 °C, the oxygen diffusion process generates a $\beta \rightarrow \alpha$(O) phase transformation when the local oxygen concentration exceeds the oxygen solubility limit within the β phase (see Zr–O phase diagram, Fig. 3).

For temperatures above ~1000–1050 °C (which correspond more or less to the zirconia phase transition temperature), the oxide tetragonal phase is formed instead of the low temperature (LT) monoclinic one. Thus, it is generally admitted that, above 1000–1050 °C and up to 1400–1500 °C, the tetragonal oxide formed is adherent and protective, even for thick scale oxide. It is admitted too that the overall cladding oxidation kinetics is parabolic, in accordance with the classical hypothesis of Wagner's theory [14]: oxide growth is controlled by thermally activated diffusion inside the oxide scale. The anionic vacancies are the predominant defects which can be found in non stoichiometric monoclinic/tetragonal zirconia.

Finally, when the temperature decreases quickly (during the final quenching stage), almost all the atomic movements stop, leading to a complex microstructure containing three phases: prior β_{Zr} phase (enriched in Fe, Cr and, potentially, H), α_{Zr} (enriched in O)

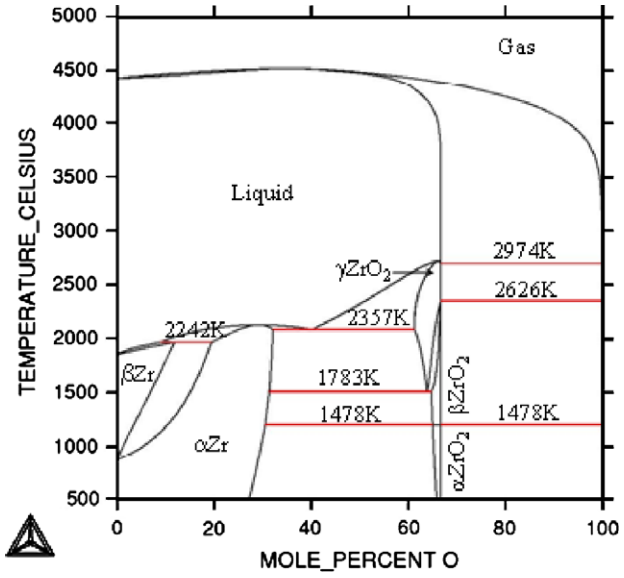

Fig. 3. Zr–O phase diagram [3] illustrating the phase transformations by the oxygen diffusion.

and oxide. The specific influence of β-stabilizing elements such as Fe, Cr and H on the PQ properties is generally neglected, except for the particular case of hydrogen [1]. Indeed the hydrogen concentration has a high influence on the HT oxidation and consequently on the residual cladding mechanical properties. Grobe et al. [15] and Brachet et al. [16] investigated the hydrogen uptakes. Grobe [15] proposed an hydrogen enrichment (close to metal/oxide interface) by the existence of cracks inside the oxide layer. Brachet et al. [16] considers this hydrogen enrichment as "unusual".

In order to anticipate fuel cladding structural evolution during the LOCA transient, several kinds of oxidation models have been elaborated for more or less simplified systems.

Debuigne [17] solved the oxidation problem in the Zr–O system. This author used an analytical resolution with the assumption of a steady-state regime and semi-infinite conditions. More recently, this analytical approach has been revisited and applied to steam oxidation of Low-Tin Zircaloy-4 in the 1100–1250 °C oxidizing temperature range [3]. However, the required steady-state hypothesis for analytical treatment limits this model to semi-infinite samples. In fact, for longer oxidation times, there is a strong influence of the finite size of the sample (due to the limited thickness of the cladding, 585 μm). This induces a progressive oxygen saturation of the inner residual β layer. Hence, such analytical models are generally limited to isothermal conditions and short times oxidation.

There are only few numerical codes developed for Zircaloy oxidation and oxygen diffusion at high temperature. Particularly, Iglesias et al. [18] proposed the FROM (Full Range Oxidation Model) code. This model was added in the nodal general simulation platform for CANDU fuel design [19] in order to reproduce the LOCA transient conditions. The FROM code solves the Fick's equations by finite difference method to simulate the oxidation of the Zy-4 alloys and the oxygen redistribution during an isothermal oxidation or an arbitrary temperature transient. This code considers non-equilibrium boundary concentrations relies on analytical expressions for the interface concentrations and the transition from two to three phases can be treated. However the results presented in [18] are focused on the thickness evolution of oxide and α layers. The oxygen diffusion profiles are not shown in details for the calculation of oxygen concentration in the β phase. So even if the effect of finite size samples and the supersaturation in the β phase seems to be solved by the FROM code, such results are not presented.

For the analysis of mechanical properties, the possibility of an embrittlement based on residual thickness of prior β_{Zr} layer with low oxygen content needs an appropriate calculation tool. In this frame a new tool has been developed. This tool is an adaptation of the "EKINOX" [5] numerical code, coupled with the "ZIRCOBASE" Thermodynamic database [4]. These calculations are focused on the effect of the finite size samples and the effect of the equilibrium interface concentration (which varies with the alloying element concentrations) on the calculation of PQ mechanical properties of fuel claddings. The first calculations presented in this paper are only for isothermal oxidation cases.

3. Calculation tools

3.1. ThermoCalc-ZIRCOBASE

ThermoCalc [20] is a powerful software which allows the calculations of different thermodynamic parameters in multi-alloyed materials. During the past few years, CEA (Commissariat à l'Energie Atomique) has been involved in the development of a thermodynamic database named "ZIRCOBASE"[4], using ThermoCalc software formalism. It performs thermodynamic calculations in multi-component Zr base alloys.

3.2. EKINOX

"EKINOX" (Estimation Kinetics Oxidation) [5] is a model originally developed to simulate the growth of an oxide layer during high temperature oxidation of Ni alloys. The model is based on an original numerical treatment taking into account both oxide growth and the relative motion between the substrate lattice and the oxide lattice due to the elimination of vacancies at the interface, assuming a non uniform dislocation distribution in the metal. In the present work, this model was adapted in order to simulate high temperature oxidation in Zr alloys.

3.3. TQ

TQ is an interface program with a set of subroutines and/or functions written in Fortran. It allows the linking of a thermodynamic database (ThermoCalc formalism) with any program written in FORTRAN. In the present study the connexion TQ-ZIRCOBASE allows the determination of equilibrium concentrations at the different interfaces, taking into account the nominal chemical composition of the cladding materials.

3.4. Corresponding diffusion–reaction model

Modeling the kinetics of phase transformation and the oxygen diffusion profile inside the cladding tube implies a simplification of the system. Only one kind of zirconia is considered and the initial condition systematically assumes a layer of α phase in the β substrate. So the model is adapted to predict oxygen diffusion profiles at high temperatures (~900–1800 °C). During the oxidation of the β_{Zr} phase, the diffusion of oxygen and growth of α(O) phase (in the outer part of the cladding at the metal/oxide interface) are the main evolutions considered in the metallic substrate. The oxide growth and the α phase growth can then be treated as a 1-Dimension (1-D)-planar geometry diffusion problem with fixed conditions at mobile interfaces. The following hypotheses are required:

(1) The system considered is always constituted by three distinct phases forming three adjacent layers: oxide, α phase, β phase.
(2) The only diffusing component considered is oxygen.
(3) Inside the oxide, oxygen diffuses across the oxide layer via the anionic vacancies. Whereas in the metal, the diffusion of oxygen takes place via an interstitial mechanism both in the α_{Zr} and in the β_{Zr} structures.
(4) Only volume diffusion is considered (i.e., no significant contribution of grain boundaries).
(5) Local thermodynamic equilibrium conditions are assumed at all interfaces: the oxygen and zirconium chemical potentials are equal on both sides of the interface.
(6) In a given phase, the oxygen diffusion coefficient is independent of the local concentration of oxygen.

From hypothesis 5 the boundary conditions for the system (Fig. 4) can be directly written as follows: the concentrations at the interfaces – respectively noticed: *vap*/*ox*, *ox*/α, and α/β are the fixed equilibrium concentrations which can be deduced from the binary Zr–O system or from ThermoCalc-ZIRCOBASE for Zircaloy-4. At each time *t*, the following boundaries conditions are fulfilled $c(0,t) = ox/C_{vap}$:

$$c_{ox}(\xi_1, t) = C_{ox/\alpha} \quad (1)$$

$$c_{\alpha}(\xi_1, t) = C_{\alpha/ox} \quad (2)$$

$$c_{\alpha}(\xi_2, t) = C_{\alpha/\beta} \quad (3)$$

$$c_{\beta}(\xi_2, t) = C_{\beta/\alpha} \quad (4)$$

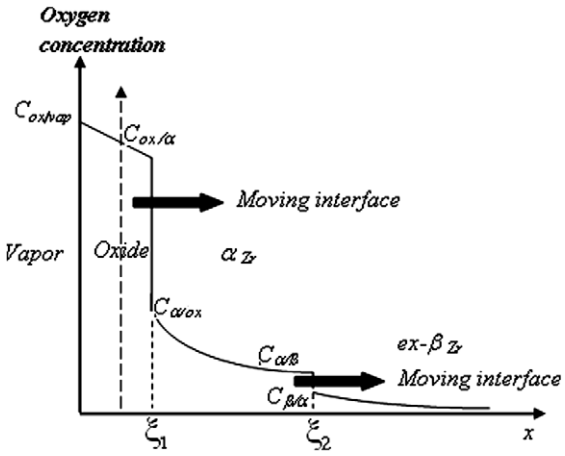

Fig. 4. Schematic diagram of Zircaloy-4 oxidized at temperature above the $\alpha-\beta$ transition temperature.

where ξ_1 and ξ_2 are respectively the oxide ox/α interface position and the α/β interface position.

Diffusion phenomena in each phase are described by the classical (1-D) Fick's laws:

$$J = -D\frac{\partial c}{\partial x} \tag{5}$$

$$\frac{\partial c}{\partial t} = D\frac{\partial^2 c}{\partial x^2} \tag{6}$$

The growth rate of the α phase is linked to the velocity of the α/β interface, which can be deduced from the oxygen mass balance at the α/β interface:

$$(C_{\alpha/\beta} - C_{\beta/\alpha})\frac{\partial \xi_2}{\partial t} = D_\alpha \frac{\partial c_\alpha}{\partial x}\bigg|_{\xi_2} - D_\beta \frac{\partial c_\beta}{\partial x}\bigg|_{\xi_2} \tag{7}$$

where c_β and c_α are the oxygen concentrations in β and α phase, respectively; D_β and D_α are the oxygen diffusion coefficients in β and α phase, respectively and ξ_2 is the α/β interface position in the system.

Considering the fact that the oxide growth is only due to anionic diffusion inside the oxide, the oxide growth only results from the ox/α interface motion which follows a similar equation but taking into account the volume change due to the Pilling-Bedworth ratio, $PBR = \Omega_{ZrO_2}/\Omega_{\alpha(Zr)}$.

In the reference frame chosen Fig. 4 – the interface position ξ_1 is equal to the metal recession due to the oxide growth

$$(C_{ox/\alpha} - C_{\alpha/ox})\frac{\partial \xi_1}{\partial t} = D_{ox}\frac{\partial c_{ox}}{\partial x}\bigg|_{\xi_1} - D_\alpha \frac{\partial c_\alpha}{\partial x}\bigg|_{\xi_1} \tag{8}$$

The oxide growth is then linked to the previous equation by:

$$\frac{\partial e_{ox}}{\partial t} = PBR\frac{\partial \xi_1}{\partial t} \tag{9}$$

where e_{ox} is the thickness of the oxide layer.

In the previous analytical model [3], the set of equation, from Eqs. (1)–(6), was analytically solved adding a quasi-steady-state hypothesis, and assuming parabolic rate constants for interfaces motions.

In the EKINOX code, the set of differential equations, Eqs. (1)–(8), is solved with a numerical time integration based on explicit finite difference and with an adequate numerical algorithm to tackle the moving interface boundaries issue.

4. The numerical model EKINOX-ZIRCOBASE applied to Zr alloys oxidized at high temperatures

4.1. General description

The numerical code EKINOX is a one dimensional model that simulates the growth of an oxide layer using a simple explicit finite differences method for the time integration algorithm [5]. To tackle the problem of oxygen diffusion inside the substrate in the case of Zr base alloys, an adaptation of the EKINOX code has been performed. First, a non-null oxygen equilibrium concentration in the substrate has been added. Second, an additional interface has been included into the substrate in order to simulate the $\beta \rightarrow \alpha$ phase transformation.

The substrate is divided into n_s layers of equal initial thicknesses (Fig. 5).

The substrate of metal ($\alpha(O)_{Zr}$ and β_{Zr}) extends from 1 to $n_{i1}+1$ slab and the oxide scale extends from the slab n_{i1} to the slab number n_s. In the oxide, two sub-lattices are considered for the cations and for the anions, whereas only one lattice is considered in the metal. Each sub-lattice is filled either by the corresponding chemical species k (metal, oxygen) or by the corresponding vacancies V_k.

4.2. Equations governing the evolution of the concentration profiles

Species transport is calculated from slab to slab with the explicit treatment of vacancy fluxes, following Fick's first law:

$$J^n_{V_k} = -\frac{D^n_{V_k}}{\Omega^n}\frac{X^{n+1}_{V_k} - X^n_{V_k}}{\frac{e^n+e^{n+1}}{2}} \tag{10}$$

Eq. (10) gives the flux $J^n_{V_k}$ of vacancies V_k from slab n to $n+1$ in the reference frame corresponding to the nature of the considered slab n. e^n is the thickness of the slab n, $X^n_{V_k}$ is the concentration in site fraction of the vacancies V_k in the slab n, $D^n_{V_k}$ is the diffusion coefficient of the V_k vacancies in the slab n and Ω^n is the molar volume of slab n. Then, the rate of change of the concentration $\dot{X}^n_{V_k}$ of vacancies V_k in the slab n is given by the Eq. (11). A mirror condition is considered in the slab 1 which means that the model calculates the oxidation of a finite size sample.

$$\dot{X}^n_{V_k} = \frac{dX^n_{V_k}}{dt} = -\Omega^n\frac{J^n_{V_k} - J^{n-1}_{V_k}}{e^n} \tag{11}$$

4.3. Interface motion

For the slabs beside the interfaces (n_{i1}, $n_{i1}+1$, n_{i2}, $n_{i2}+1$ and n_s), the conservation equation (Eq. (11)) leads to a thickness variation of the slabs. The corresponding variation with time of the slab thickness $\dot{e}^{ni+1}_1$ and $\dot{e}^{ni+1}_2$, is given by Eqs. (12) and (13). These variations are directly in function of the oxygen flux at the interfaces (J^{ni-1}_0, J^{ni+1}_0, for i_1 and i_2) and the oxygen equilibrium concentration at the different interfaces ($C^{ox/\alpha}_0, C^{\alpha/ox}_0, C^{\alpha/\beta}_0$ and $C^{\beta/\alpha}_0$). The anionic

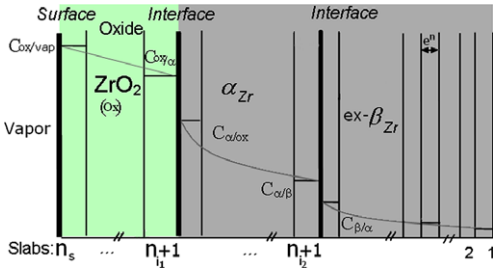

Fig. 5. Schematic representation of the concentration profile.

oxide growth leads to a recession of the metal layer thickness in the ratio of the molar volumes, that is to say the Pilling-Bedworth Ratio of the oxide type MO_γ:

$$\dot{e}^{n_{i_1}+1} = \frac{\Omega^{n_{i_1}+1}}{\gamma}\frac{J_o^{n_{i_1}-1} - J_o^{n_{i_1}+1}}{C_o^{ox/\alpha} - C_o^{\alpha/ox}} \tag{12}$$

$$\dot{e}^{n_{i_2}+1} = \Omega^{n_{i_2}+1}\frac{J_o^{n_{i_2}-1} - J_o^{n_{i_2}+1}}{C_o^{\alpha/\beta} - C_o^{\beta/\alpha}} \tag{13}$$

The implementation of the algorithm for moving boundaries is described in [21].

5. Results

5.1. Initial conditions

In order to perform an EKINOX simulation, the initial concentration profile of the system is needed as an input data. Since EKINOX does not treat germination but only the growth of the oxide and the α phase, thin layers of these two phases are already pre-existing at $t = 0$. Hence the chosen value for the initial condition: $e_{ox} = 1.93$ μm and $e_\alpha = 1.93$ μm and the initial concentration profile is as follows:

- In the oxide, a linear profile from $C_{vap/ox}$ to $C_{ox/\alpha}$ is assumed.
- In the α phase, the initial profile is uniform in the whole phase and taken at the equilibrium value of the α/β interface, except at the oxide/α phase interface where the equilibrium concentration $C_{ox/\alpha}$ is respected.
- In the β phase, the initial profile is uniform in the whole phase and taken at the nominal oxygen composition of Zy-4 alloy – 0.74 at.% except at the α/β phase interface where the equilibrium concentration $C_{\beta/\alpha}$ is respected.

5.2. Input data for the simulation

Two types of input data are needed for the EKINOX calculations: the equilibrium concentration at each interface and the diffusion coefficient in each phase. The first ones can be seen as purely thermodynamic data and the second ones as kinetics data.

5.3. Thermodynamic data set

Chung and Kassner [22] have investigated the zirconium-rich portion of the pseudo-binary Zircaloy-4/oxygen phase diagram. At $T > 1280$ K, these authors expressed empirically the equilibrium concentrations between the β and α phases as follows:

$$\ln C_{\beta/\alpha} = 5.02 - \frac{8220}{T} \tag{14}$$

$$\ln C_{\alpha/\beta} = -2.28 + 0.535 \cdot \ln(T - 1083) \tag{15}$$

where $C_{\beta/\alpha}$ and $C_{\alpha/\beta}$ are the equilibrium oxygen concentration in wt.% at the β and α-phase boundaries respectively at a given temperature T (in Kelvin).

Equilibrium oxygen concentrations can also be calculated using ThermoCalc and the ZIRCOBASE database [4]. These concentrations have been calculated for both Zr–O system and the Zircaloy-4 alloy, in the [1100–1250 °C] temperature range. The typical chemical composition of Low-Tin Zircaloy-4 alloy used for ThermoCalc calculations is given in Table 1.

Table 2 summarizes the equilibrium concentrations obtained from Chung–Kassner (C–K) expressions and from ThermoCalc-ZIRCOBASE (TC), considering either Zr–O or Zy-4 systems.

Table 1
Typical chemical composition of the Low-Tin Zircaloy-4 alloy considered for the calculation.

Alloying elements	Sn	Fe	Cr	O
Wt.%	1.30	0.20	0.09	0.138

Table 2
Interface equilibrium oxygen concentrations (in atomic fraction) of Zr–O or Zircaloy-4 at 1100, 1200 and 1250 °C, calculated from Chung–Kassner (C–K) or ThermoCalc-ZIRCOBASE (TC).

T °C		$C_{\beta/\alpha}$		$C_{\alpha/\beta}$		$C_{\alpha/ox}$	
		Zy-4	Zr–O	Zy-4	Zr–O	Zy-4	Zr–O
1100	TC	0.0174	0.0224	0.0859	0.0809	0.2953	0.3011
	C–K	0.0213		0.1100			
1200	TC	0.0279	0.0336	0.1086	0.1033	0.2998	0.3053
	C–K	0.0316		0.1267			
1250	TC	0.0322	0.0393	0.1175	0.1129	0.3021	0.3072
	C–K	0.0376		0.1344			

Table 3
Diffusion coefficients in α_{Zr}, β_{Zr} and ZrO_2 at 1100, 1200 and 1250 °C.

T °C	D_α (cm^2/s)	D_β (cm^2/s)	D_{ox} (cm^2/s)
1100	2.48×10^{-8}	8.44×10^{-7}	3.99×10^{-7}
1200	8.50×10^{-8}	1.55×10^{-6}	9.21×10^{-7}
1250	1.48×10^{-7}	2.05×10^{-6}	1.35×10^{-6}

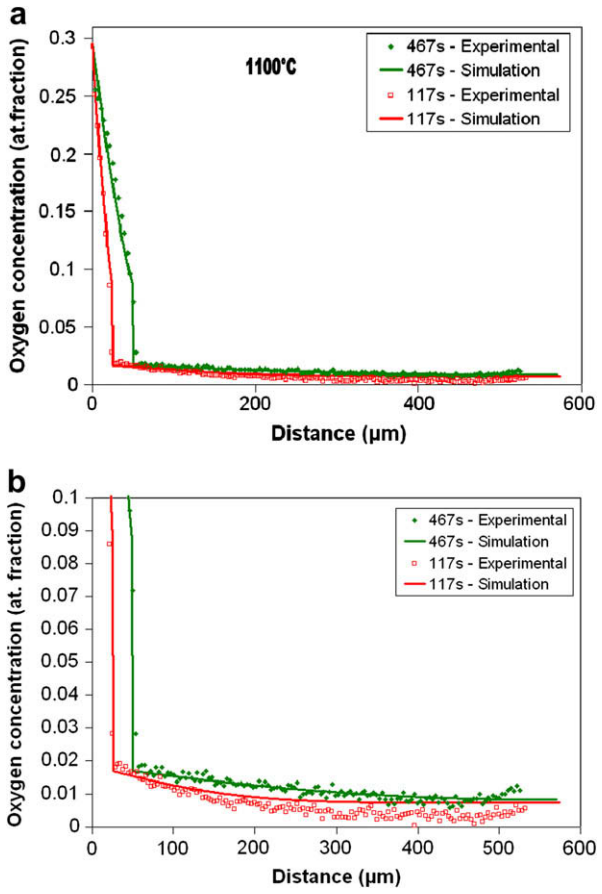

Fig. 6. (a) Comparison between experimental [1] and calculated O diffusion profiles in Low-Tin Zircaloy-4 at 1100 °C. (b) Blow-up of (a).

5.4. Kinetic data set

The set of diffusion coefficients used for the EKINOX simulations are presented in Table 3.

For the ZrO_2 and β phase, the diffusion coefficients have been calculated from the diffusion parameters of the Ma et al. [3]. These parameters were deduced from [23] (beta-phase) and from [24,25] (ZrO_2-phase).

For the α phase, a different strategy has been chosen: a parametric study of the model has revealed that diffusion coefficient in the α phase is the kinetic parameter that has the more significant influence on the α/β interface motion. The diffusion coefficient for the α phase has been then chosen in order to obtain the best agreement for the calculated α/β phase position with existing experimental one.

Hence the D_α values presented in Table 3 are the ones that give the best agreement between experimental and calculated $\alpha(O)/\beta$ phase locations.These coefficients were determined by performing several simulations with different diffusion parameters.

5.5. Comparison between EKINOX simulations and experimental oxygen diffusion profiles

The calculated oxygen diffusion profiles in the α and β phases of Low-Tin Zircaloy-4 are presented in the temperature range [1100–1250 °C] for different times. These profiles have been obtained via EKINOX calculations using TC values from Table 2 and kinetic parameters given in Table 3. Figs. 6–8 show a comparison of experimental data [1] with EKINOX simulations at 1100 °C, 1200 °C and 1250 °C.

The different simulation profiles are within the experimental quoted errors (around 1×10^{-2} atomic fraction) except for the longest oxidation time at 1200 °C, due to achievement of the β phase

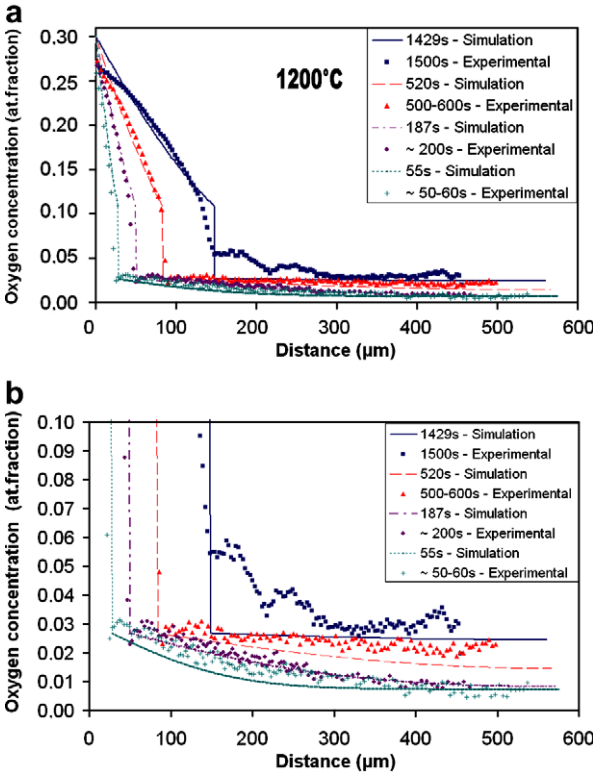

Fig. 7. (a) Comparison between experimental [1] and calculated O diffusion profiles in Low-Tin Zircaloy-4 at 1200 °C. (b) Blow-up of (a).

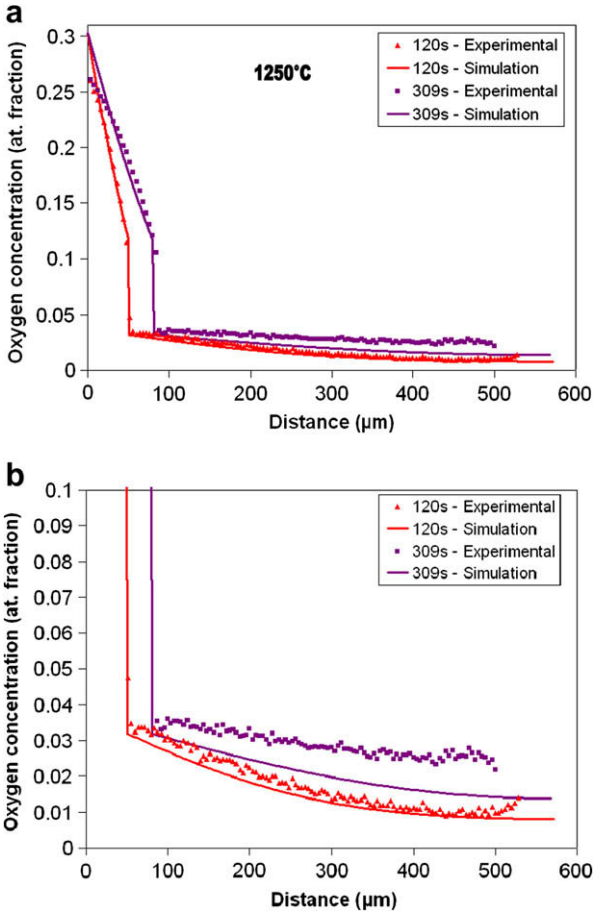

Fig. 8. (a) Comparison between experimental [1] and calculated O diffusion profiles in Low-Tin Zircaloy-4 at 1250 °C. (b) Blow-up of (a).

saturation which induces $\alpha(O)$ incursions within the inner prior-β layer. Additionally, the determination of the experimental equilibrium concentration at the α/ox interface is quite difficult. Considering these points, simulations appear to be in good agreement with the experimental data.

6. Discussion

6.1. Kinetic parametrization

EKINOX simulations offer a new tool to determine accurately diffusion coefficients in the metallic phases. Indeed, the α/β interface displacement is directly linked to time integration of Eq. (7) which can be rewritten as follows:

$$[C_{\alpha/\beta} - C_{\beta/\alpha}]d\xi_2 = (J_\alpha - J_\beta)_{\xi_2} dt \tag{16}$$

where $C_{\alpha/\beta}$ and $C_{\beta/\alpha}$ are the equilibrium oxygen concentrations at the interface, in the α and β phases respectively, J_α and J_β are the α and β phase fluxes and $d\xi_2$ is the α-growth in dt time.

The Eq. (16) shows that the interface motion in the EKINOX simulations depends upon diffusion coefficient parameters of α and β phases via J_α and J_β. On the contrary, in the previous analytical models [3], the position of the interface is linked to a supplementary input data: K_α, the experimental parabolic rate constant for the $\alpha(O)$ phase.

Furthermore some simulations have shown that, numerically, the α phase kinetic parameters had a more significant influence on the interface motion, due to J_α dependence upon both: $\beta \rightarrow \alpha$

Table 4
Comparison of the oxygen diffusivities at 1200 °C.

O diffusivities in α_{Zr}	D_0 (cm^2/s)	Q (kJ/mol)	$D_{1200\,°C}$ (cm^2/s)
Ma et al. [3]	1.543	201.55	1.09×10^{-7}
Pawel et al. [25]	3.920	213.18	1.07×10^{-7}
This work	1.865	206.90	8.50×10^{-8}

and $\alpha \rightarrow$ oxide transformations. Consequently, the choice of adequate kinetic variables in the α phase strongly influences the results of EKINOX calculations. To illustrate this point, three simulations using different sets of α-kinetic data were performed. The first and the second values of D_α were extracted from [3,25] and the third one was obtained using the set of kinetic data adjusted in the present study. The different sets of data are summarized in Table 4. The results are shown in Fig. 9 where experimental data from [1] have been also added. The EKINOX simulations using this new set of kinetic data shows a better agreement with the experimental data than the simulations using kinetic parameters from [3] and [25] which overestimates the α growth rate.

Thanks to several experimental diffusion profiles for the Low-Tin Zircaloy-4 at different times and temperatures [1], the α/β interface position can be accurately measured and the diffusion coefficient in the α-phase has been chosen in order to reproduce the experimental α/β interface position in the [1100–1250 °C] temperature range.

The Arrhenius plot (Fig. 10) determined from EKINOX diffusion simulations can be expressed by the Eq. (17). The activation energy value (207 kJ) is in good agreement with previous works [3,25].

$$D_\alpha(T) = 1.8652 \cdot \exp\left(\frac{-207\ \text{kJ}}{R \cdot T}\right)(\text{cm}^2/\text{s}) \tag{17}$$

Contrary to the oxygen profiles in the α phase and the β phase which require accurate WDS procedure to be quantitative, the α/β interface position can be easily experimentally located with a good accuracy. Hence EKINOX calculations offer an interesting tool to estimate the overall effective diffusion coefficient from oxidation tests on Zr base alloys, by simply considering the respective ZrO_2, α(O) and β phase thicknesses, which can be easily and accurately obtained experimentally.

6.2. Comparison between numerical and analytical solutions

In order to evaluate the improvement obtained by non-stationary calculations using EKINOX simulations, the simulated oxygen diffusion profiles inside HT oxidized cladding tubes have been compared to previous analytical models [3]. The data needed in the analytical solution are the following ones:

- The experimental, parabolic growth rate constants K_p and K_α, respectively for oxide and α phase.
- The equilibrium oxygen concentrations at the different interfaces.
- Diffusion coefficients in the α and β phases.
- Moreover, the analytical solution is applied to semi-infinite systems (see [3] for more details).

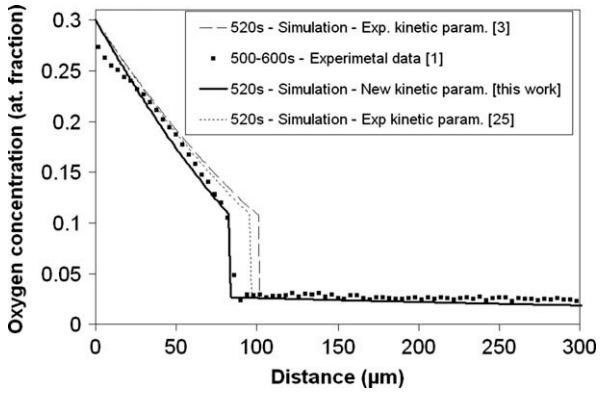

Fig. 9. Simulations and experimental data of O diffusion profiles in α_{Zr} and β_{Zr} at 1200 °C.

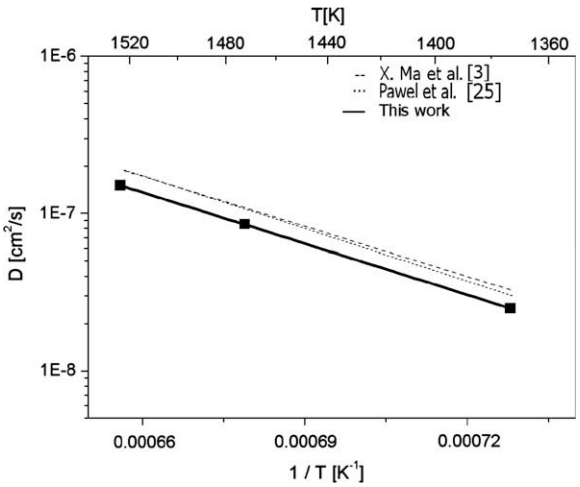

Fig. 10. Arrhenius diagram of O diffusion in α_{Zr}.

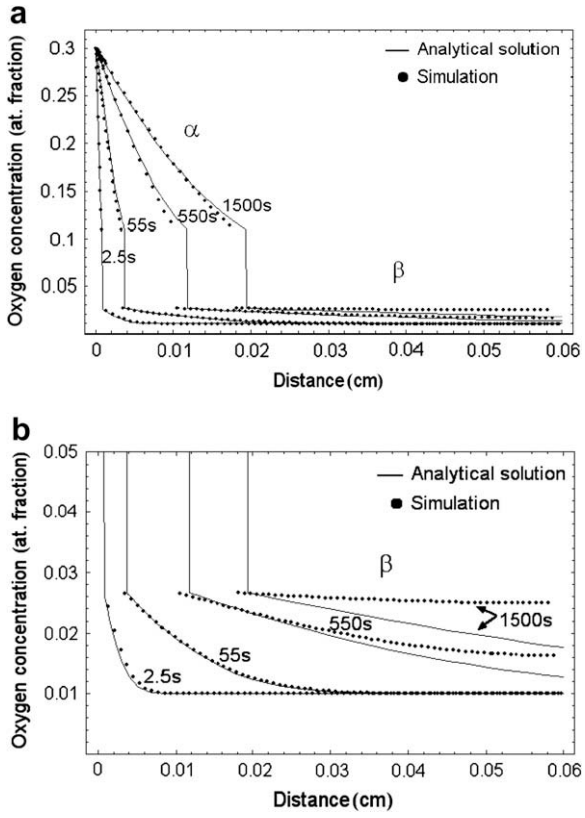

Fig. 11. (a) Comparison between O diffusion profiles obtained using the analytical model [3] and the EKINOX numerical simulations. (b). Blow-up of Fig. 11a.

Ma et al. [3] applied the steady-state analytical solution for oxidations at 1200 °C for various simulation times. Fig. 11 gives for the same set of thermodynamic and kinetic data, a comparison of diffusion profiles obtained by EKINOX simulation and with the analytical solution. The analytical calculations of the O profiles presented in Fig. 11 use the parabolic rate constant for α_{Zr} phase and oxide phase from [3].

For short simulation times, the analytical and numerical diffusion profiles are in good agreement. For longer simulation times (beyond 200 s), a discrepancy appears which is due to the effect of the finite size sample: the increase in the oxygen concentration profile at the right-hand side of Fig. 11 revealed an oxygen enrichment in the inner part of wall thickness of the cladding, due to the zero-flux limit conditions at the inner side of the clad (right side of the Fig. 11a). Thus, beyond 200 s at 1200 °C, there is an effective flattening of the profile up to achievement of full oxygen saturation of the inner β layer. This decrease of the oxygen concentration gradient lowers the α/β interface velocity. This effect is well reproduced by EKINOX calculation but not by the analytical model.

This phenomenon illustrates the importance of taking into account a finite size system, allowed by the EKINOX simulations thanks to the non-steady-state hypothesis.

6.3. Influence of equilibrium concentrations at the different interfaces on the oxygen diffusion profile

In order to evaluate the influence of thermodynamic data (i.e., oxygen solubilities) on the calculated oxygen diffusion profiles, new calculations have been done using, respectively, Chung–Kassner and ThermoCalc values for Zircaloy-4 and binary (pure) Zr–O as given in Table 2.

Fig. 12 shows that the choice of the thermodynamic data set has a strong influence on the diffusion profiles, mainly in the β phase. This result points out the necessity to take into account the nominal composition of the industrial alloys (main alloying chemical element and/or impurities) for the calculation of equilibrium oxygen concentrations, in order to better evaluate the oxygen diffusion profiles evolutions in HT oxidized cladding materials.

6.4. Evaluation of the overall ductile-to-brittle transition from EKINOX simulations

As mentioned earlier, considering that both: ZrO_2 and α(O) phases, are fully brittle at room temperature (RT), previous LOCA studies have shown that the overall PQ ductility/toughness of HT oxidized Zr base claddings can be directly correlated to the oxygen diffusion profile within the residual inner prior-β phase layer (as a first step, without taking into account the additional effect of H – hydrides content). To derive the "critical" oxidizing time at 1200 °C on as-received Low-Tin Zircaloy-4, Portier et al. [26] have considered a critical impact energy value of 0.05 J/mm^2 for the (macroscopic) ductile-to-brittle transition. Tests show that this value is achieved for a typical weight gain of ~18 mg/cm^2, that is for an oxidation time of ~17 min at 1200 °C. Indeed, the previous PQ mechanical tests have shown the existence of a ductile-to-brittle failure mode transition at RT for a critical oxygen concentration close to 0.4 wt.% (~2.2 at.%). It means that, beyond this critical oxygen concentration value, the prior-β phase displays a "quasi-brittle" failure mode, with no significant plastic strain before rupture.

Calculations have been performed in order to predict the critical oxidizing time at 1200 °C considering the critical oxygen concentration of 0.4 wt.%, corresponding to the moment where the β-prior phase should become completely brittle (and consequently the overall cladding tube). This corresponds to the time when the oxygen concentration profile goes ahead 0.4 wt.% within the full residual prior-β phase layer. Table 5 presents the various calculated values for the critical oxidizing time obtained using respectively analytical model and with EKINOX calculations considering the different thermodynamic data sets presented in Table 2. These values are compared to the experimental one taken from [26]. The value calculated with the analytical model strongly overestimates the critical time. This is not surprising considering the fact that the model cannot take into account the finite size of the sample. In contrast, the value calculated with EKINOX simulation and thermodynamic data sets taken from Zy-4 ZIRCOBASE database offers a good estimation of the critical time.

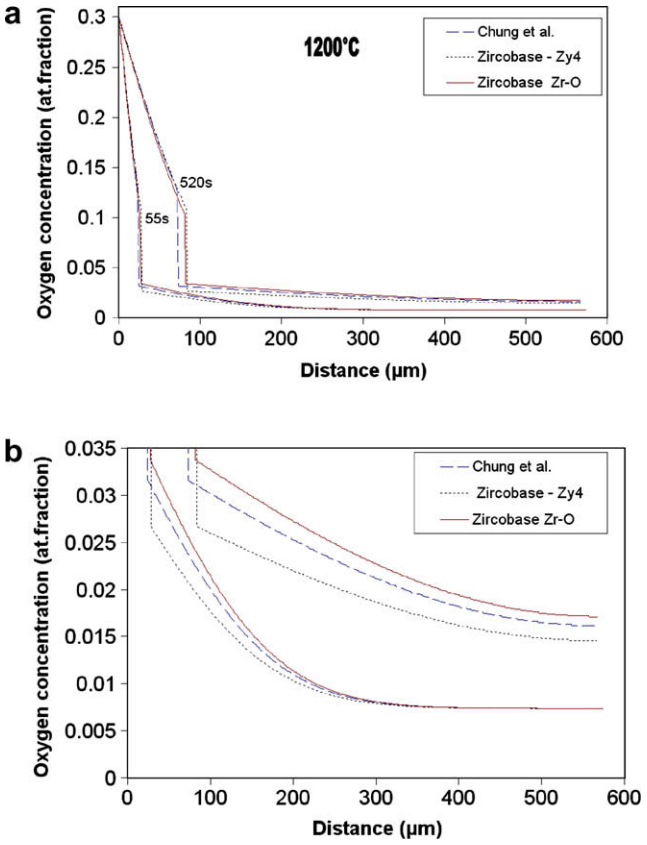

Fig. 12. (a) Simulation of O diffusion profiles in α_{Zr} and β_{Zr} at 1200 °C using different sets of thermodynamic data (Chung and Kassner [22] and ZIRCOBASE [4]). (b) Blow-up of the simulated O diffusion profiles in β_{Zr} at 1200 °C.

Table 5
Calculation of critical time oxidation for ductile-to-brittle transition at 1200 °C.

Analytical	EKINOX–ZIRCOBASE Zy-4	EKINOX-Chung and Kassner	EKINOX–ZIRCOBASE Zr-O	Experimental
41 min	17.8 min	13.6 min	12.2 min	17 min

7. Conclusions

In this work, a new tool has been developed. It is constituted by the diffusion code EKINOX adapted for Zr base alloys and the ZIRCOBASE thermodynamic database (ThermoCalc formalism) coupled via the TQ Interface.

This tool is able to simulate oxygen diffusion profiles in α and β phases of Zr base alloys due to HT oxidation in the temperature range [1100–1250 °C].

This numerical model simulates the α/β interface position during the $\beta_{Zr} \rightarrow \alpha_{Zr}$ phase transformation. This is possible only with the diffusion coefficient information in each phase and without the addition of any other kinetic parameters.

The influences of thermodynamic and kinetic parameters on the calculated profiles, specifically in the α phase, have been estimated. Thus, a re-identification of α diffusion parameters has been performed, showing good agreements with previous works.

Compared to an analytical model, EKINOX model shows a better agreement with experimental data thanks to the consideration of a finite size sample and to the non steady-state hypothesis.

At last, for Low-Tin Zircaloy-4 steam oxidation at 1200 °C, the diffusion time for the ductile-to-brittle transition was predicted showing a good agreement with the experimental determination.

Further work in Low-Tin Zircaloy-4 industrial alloys:

- The simulations will be performed in order to evaluate the hydrogen effects on oxygen diffusion profiles.
- New improvements in the EKINOX code will be performed in order to allow the simulations of anisothermal oxygen diffusion in LOCA temperature–times range for Zr base alloys.
- EKINOX will be adapted in order to solve the case of oxide dissolution in the substrate which cannot be treated by an analytical solution that assumes a parabolic growth kinetic for the α phase.

References

[1] J.C. Brachet, V. Vandenberghe, et al., American Society for Testing and Materials 5 (5) (2008) 91–118. paper ID JAI101116.
[2] J. Kim, M. Lee, B. Choi, Y. Jeong, Journal of Nuclear Materials 362 (2007) 36–45.
[3] X. Ma, C. Toffolon-Masclet, T. Guilbert, D. Hamon, J.C. Brachet, Journal of Nuclear Materials 377 (2008) 359–369.
[4] N. Dupin, I. Ansara, C. Servant, C. Toffolon, C. Lemaignan, J.C. Brachet, Journal of Nuclear Materials 275 (1999) 287–295.
[5] C. Desgranges, N. Bertrand, K. Abbas, D. Monceau, D. Poquillon, Materials Science Forum 461–464 (2004) 481–488.
[6] N. Bertrand, C. Desgranges, M. Nastar, G. Girardin, D. Poquillon, D. Monceau, Materials Science Forum 595–598 (2008) 463–472.
[7] A. Sawatzky, American Society for Testing and Materials 681 (1979) 479–497.
[8] L. Baker, L. Just, ANL-6548, vol. 111, Argonne National Laboratory, Argonne, 1962.
[9] V.F. Urbanic, T.R. Heidrick, Journal of Nuclear Materials 75 (1978) 251–261.
[10] D.O. Hobson, P.L. Rittenhouse, Oak Ridge National Laboratory, ORNL-4758, 1972.
[11] H. Ocken, R.R. Biederman, C.R. Hann, R.E. Westerman, 4th Int. Symp. "Zirconium in the Nuclear Industry", vol. 681, American Society for Testing and Materials Special Technical Publications, 1979, pp. 514–536.
[12] H. Ocken, Nuclear Technology 47 (1980) 343–357.
[13] J.-C. Brachet, L. Portier, D. Hamon, P.H. Trouslard, S. Urvoy, V. Rabeau, in: Proceeding of Special Expert Group Fuel Safety Margins Meeting, 2004.
[14] C. Wagner, Corrosion Science 9 (1969) 91–109.
[15] M. Groβe, E. Lehmann, M. Steinbrück, G. Kühne, J. Stuckert, Journal of Nuclear Materials 385 (2009) 339–345.
[16] J.-C. Brachet, V. Vandenberghe, Journal of Nuclear Materials 395 (2009) 169–172.
[17] J. Debuigne, PhD thesis, Paris University, 1966 (in French).
[18] J.C. Iglesias, D.B. Duncan, S. Sagat, H.E. Sills, Journal of Nuclear Materials 130 (1985) 36–44.
[19] B.J. Lewis, F.C. Iglesias, R.S. Dickson, A. Williams, Journal of Nuclear Materials 394 (2009) 67–86.
[20] B. Sundman, B. Jansson, J.-O. Andersson, Calculation of Phase Diagrams 9 (1985) 153–199.
[21] C. Desgranges, PhD Thesis, Université Paris XI Orsay, 1998 (also as report of the Commissariat à l Energie Atomique (CEA)-R-5805, –Saclay, Gif-sur-Yvette, France, 1998).
[22] H. Chung, T. Kassner, Journal of Nuclear Materials 84 (1979) 327–339.
[23] R. Perkins, Journal of Nuclear Materials 68 (1977) 148–160.
[24] B. Oberländer, P. Kofstad, I. Kvernes, Mat.-Wiss U. Werkstoffech 19 (1988) 190–193.
[25] R. Pawel, Journal of the Electrochemical Society 126 (1979) 1111–1118.
[26] L. Portier, T. Bredel, J.-C. Brachet, V. Maillot, J.-P. Mardon, A. Lesbros, American Society for Testing and Materials 2 (2) (2005) 896–919. paper ID JAI12468.